

the presence of biological noise in the output that makes it difficult to distinguish between the true zero error of a system with an integrator and the small error maintained by a type-0 system. What makes an integrator seem probable in this case is the fact that the forward-path gain necessary to permit a type-0 system to reduce blur to within the known range of insensitivity seems so large as to be rejected on stability grounds.

#### ACKNOWLEDGMENT

The author wishes to thank Prof. R. W. Jones for a particular inspirational conversation which led to this paper, and Prof. Jones and Prof. E. J. Bayly for the time they devoted to reading, criticism, and correction.

#### REFERENCES

- [1] G. Westheimer, "Focusing responses of the human eye," *Amer. J. Optom. and Arch. Amer. Acad. Optom.*, vol. 43, pp. 221-232, 1966.
- [2] P. J. Dallos and R. W. Jones, "Learning behavior of the eye fixation control system," *IEEE Trans. Automat. Contr.*, vol. AC-8, pp. 218-227, July 1963.
- [3] F. W. Campbell, "The accommodation response of the human eye," *Brit. J. Physiol. Optics*, vol. 16, pp. 188-203, 1959.
- [4] J. J. D'Azco and C. H. Houppis, *Feedback Control Systems Analysis and Synthesis*, 2nd ed. New York: McGraw-Hill, 1966, pp. 174-175.
- [5] C. F. Stevens, *Neurophysiology: A Primer*. New York: Wiley, 1966, p. 24.
- [6] E. F. Florey, *An Introduction to General and Comparative Animal Physiology*. Philadelphia, Pa.: Saunders, 1966, pp. 491 and 558.
- [7] M. A. Arbib, *Brains, Machines and Mathematics*. New York: McGraw-Hill, 1964, pp. 47-56.
- [8] C. E. Eyzaguirre, *Physiology of the Nervous System*. Chicago, Ill.: Year Book Medical Publishers, 1969, pp. 58-59.

# An Electrode for Recording Single Motor Unit Activity During Strong Muscle Contractions

CARLO J. DE LUCA, STUDENT MEMBER, IEEE, AND WILLIAM J. FORREST

**Abstract**—The construction of a lightweight quadrifilar needle electrode offering four monopolar and six bipolar microelectrode combinations is described. The electrode has three useful features: 1) it can record distinct individual motor unit action potentials during strong muscle contractions, 2) the frequency response curve of the electrode can be altered to a simple functional relationship within the frequency range of myoelectric signals, and 3) the electrode minimizes the subject's discomfort.

An electrolytic treatment for reducing the impedance of the electrode is described. The frequency response of 12 monopolar and 12 bipolar microelectrodes was measured 1) before the electrolytic treatment, 2) 10 min after the electrolytic treatment, and 3) 72 h after the electrolytic treatment. The Bode form was used to synthesize a simple resistance-capacitance ( $RC$ ) model for each of the three situations, giving some insight to the physical change at the tip of the electrode.

#### INTRODUCTION

A VARIETY of electrodes has been used to record myoelectric signals. They range from a sewing needle partially covered with lacquer [1] to a 14-wire needle

electrode [2]. Electrodes have customarily been designed to fulfill a particular need in an experiment.

The needle electrode described in this paper was designed to record motor unit action potential trains while inserted in a human skeletal muscle performing a contraction. This objective was achieved by limiting the pickup area of the electrode so that a minimal number of motor unit action potential trains were recorded. During weak muscular contractions a small number of motor units fire at a relatively slow rate; hence, a motor unit action potential train can easily be recorded. In a strong contraction more motor units are activated, firing at a relatively faster rate. Several microelectrodes that possess the high degree of selectivity required to record a motor unit action potential train during a strong contraction have been described in the literature [3]-[7]. Unfortunately, the previously described microelectrodes are only useful for recording from anesthetized animals because they are too brittle to withstand the tissue movement that accompanies a strong muscular contraction.

In this paper the term *electrode* refers to any transducer capable of recording myoelectric activity. The term *microelectrode* is used in its widest sense referring to any electrode capable of recording isolated neuromuscular events under specific conditions.

Manuscript received June 7, 1971; revised October 8, 1971, December 6, 1971, and March 6, 1972. This work was supported by a grant from the Medical Research Council of Canada.

C. J. De Luca is with the Department of Anatomy, Queen's University, Kingston, Ont., Canada.

W. J. Forrest is with the Department of Anatomy, Queen's University, Kingston, Ont., Canada, and the Department of Physical Medicine and Rehabilitation, Kingston General Hospital, Kingston, Ont., Canada.

### CONSTRUCTION OF ELECTRODE

The basic structure of the needle electrode is quite similar to that of the coaxial needle electrode, which is well known to electromyographers and which was introduced by Adrian and Bronk in 1929 [8]. The electrode consists of four nylon-insulated Karma wires (76 percent Ni, 20 percent Cr, Fe, Al), each with a diameter of  $25\ \mu$  fixed in a 25 gauge  $1\frac{1}{2}$ -in disposable needle. A disposable needle is used because it has a plastic stem that is light in weight and thus more comfortable when inserted. Four wires are used in construction, giving the investigator a choice of four monopolar electrodes and/or six bipolar electrodes in the event that one or more of the electrode combinations are not functioning properly. A particular monopolar or bipolar combination of the new electrode has the properties of a microelectrode.

A wire was soldered to the shaft near the stem of the disposable needle. This wire served as a ground connection for the subject and the preamplifier to which the electrode is to be connected. (An auxiliary ground can be placed on the subject for additional safety.) All four ends of two pieces of Karma wire were inserted through the needle via the shaft and out the stem forming two loops of  $\frac{1}{2}$  cm each at the distal end of the shaft. The needle was secured to a three-dimensional micro-manipulator. A piece of nylon-insulated Karma wire  $50\ \mu$  in diameter was looped through the other loops so as to exert tension on them. The ends of all the wires were fastened to clamps. The intersection of the loops was positioned approximately 1 cm from the distal end of the shaft. Sufficient tension was exerted on the wires to ensure that all wires were taut. The micromanipulator was adjusted until the four ends of the Karma wires in the shaft were closely packed at the center of the beveled tip of the shaft. A dissecting microscope (40X) focused on the tip of the shaft was used to ensure that the four wires were approximately  $50\ \mu$  apart and formed the configuration of a square. An exaggerated version of this arrangement can be seen in Fig. 1. By careful manipulation, it is possible to position the wires in various configurations.

The wires were secured by applying a drop of epoxy cement at the tip of the shaft. When the epoxy cement was dry, the tip of a new number 11 rib-back scalpel blade was used to cut the wires and the adjoining epoxy on a plane perpendicular to the length of the shaft as shown in Fig. 2. It is imperative that the cut be made with one continuous follow-through motion, so as not to disturb the position of the wires. Female Amphenol Relia-Tac 220-S02 multipurpose connectors were soldered to the four Karma wires protruding from the stem of the needle. The four connectors were secured in the stem of the needle with epoxy cement. The completed electrode is shown in Fig. 3.

### IMPEDANCE REDUCTION

Electrodes of the type described in this paper tend to have an undesirably high impedance (and resistance) that increases the thermal noise of the electrode and requires that they be matched with preamplifiers having a high input impedance. The impedance can be effectively reduced by an electrolytic treatment described by Buchthal *et al.* [9]. In the present

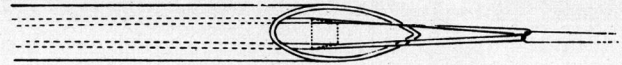


Fig. 1. Arrangement of Karma wires before applying epoxy cement.



Fig. 2. Tip of the needle electrode showing the plane of the exposed electrode wires.

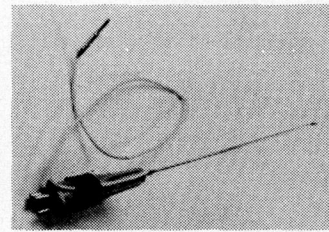


Fig. 3. Complete electrode.

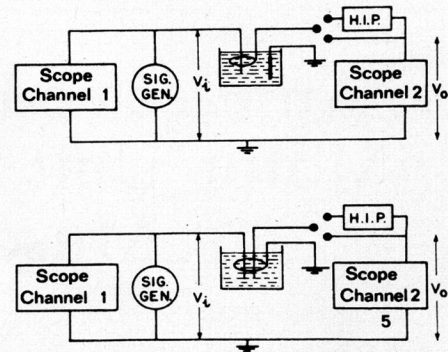


Fig. 4. Measuring arrangements for monopolar and bipolar electrodes. Channels 1 and 2 refer to a dual-channel oscilloscope.

study, the following modified electrolytic treatment was found to be most effective.

The needle electrodes were electrolytically treated after they were sterilized, prior to being inserted into the subject. Sterilization was completed after 1 h at  $130^\circ\text{C}$  in a dry-heat oven. A small electrolytic tank containing a normal saline solution (0.9 percent NaCl) and a platinum electrode was heated approximately to the boiling point of the solution. The needle electrode was immersed in the tank. The four terminals of the electrode were connected to the negative terminals of a variable power supply. The platinum electrode was connected to the positive terminal of the variable power supply. A current of 1 mA was passed through the needle electrode for a period of 1 min, effectively reducing the impedance of the microelectrode to its minimum level.

### MEASUREMENT OF ELECTRODE IMPEDANCE

Each electrode was placed in a glass electrolytic tank containing normal saline solution and a platinum electrode. Two sets of measurements were made: one set with monopolar microelectrodes, the other with bipolar microelectrodes. The two measuring arrangements are displayed in Fig. 4. An oscilloscope with a dual-trace differential preamplifier was used.

**TABLE I**  
 PHASE ANGLE OF THE MICROELECTRODE IMPEDANCE IN DEGREES: 1) BEFORE ELECTROLYSIS, 2) 72 h AFTER ELECTROLYSIS, AND 3) 10 min AFTER ELECTROLYSIS

FREQUENCY	MONOPOLAR			BIPOLAR		
	1	2	3	1	2	3
10	-55.8 ± 22.2	-41.6 ± 12.1	-46.7 ± 12.9	-46.4 ± 19.5	-39.5 ± 11.7	-55.6 ± 11.4
100	-68.7 ± 17.9	-52.2 ± 14.6	-59.1 ± 12.7	-56.5 ± 23.7	-49.2 ± 16.1	-57.7 ± 8.3
1 k	-83.3 ± 10.5	-33.5 ± 13.8	-41.7 ± 22.4	-66.7 ± 14.8	-32.3 ± 11.9	-40.0 ± 10.5
10 k	-81.7 ± 4.4	-38.3 ± 19.5	-27.1 ± 15.8	-82.5 ± 1.5	-39.9 ± 15.8	-23.6 ± 8.6
100 k	-80.7 ± 14.9	-53.0 ± 23.5	-20.2 ± 11.8	-84.5 ± 6.1	-60.8 ± 19.9	-30.6 ± 16.1

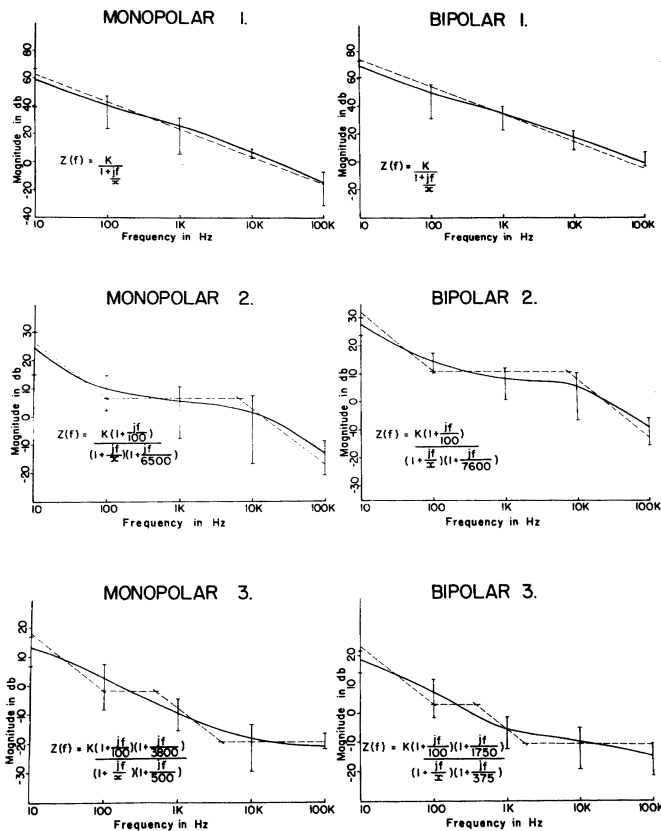


Fig. 5. Magnitude of the microelectrode impedance in decibels (0 dB = 1 MΩ): 1) before electrolysis, 2) 72 h after electrolysis, and 3) 10 min after electrolysis.

Both monopolar and bipolar microelectrodes were measured at three different times: before the electrolytic treatment, 10 min after the electrolytic treatment, and 72 h after the electrolytic treatment. An untreated electrode invariably had a high impedance, which was measured with a high impedance probe (10 MΩ, 14 pF) on channel 2 of the oscilloscope (see Fig. 4).

Twelve different needle electrodes were used for the measurements. One monopolar and one bipolar combination for each needle electrode was chosen according to random tables. Voltage magnitude and phase readings were taken at 10, 10<sup>2</sup>, 10<sup>3</sup>, 10<sup>4</sup>, and 10<sup>5</sup> Hz for each combination. Attempts at tak-

ing measurements below 10 Hz were unsuccessful because the output signal was too small and the electrode noise too large. All measurements were taken with a 10-mV peak-to-peak sinusoidal voltage across the microelectrode. This value was chosen because it was the smallest voltage that could be used consistently to obtain readings at all the measured frequencies. The impedance of the needle electrodes varies inversely with the measuring voltage [10]. Therefore, the impedance had to be measured at a voltage that was equal to, or comparable to the voltage to which the microelectrodes would be subjected during experimental conditions.

**FREQUENCY RESPONSE AND MODEL OF MICROELECTRODES**

The calculated means and standard deviations of the magnitude and phase of the measured impedances are drawn in Fig. 5 and listed in Table I, respectively. The frequency response of both the monopolar and the bipolar microelectrodes can be approximated by Bode plots; thus an equation for the microelectrode impedance as a function of frequency can be obtained. In all cases, there appears to be a pole below 10 Hz and a zero above 100 kHz. The frequency spectrum of the myoelectric signal has a substantial amount of energy below 10 Hz and an unmeasurable amount of energy above 100 kHz [11]. Therefore, the zero above 100 kHz has no practical importance. The critical frequency below 10 Hz is represented by *x* in the Bode equations on the graphs shown in Fig. 5. The values of the Bode gain *K* and the critical frequency *x* can be extrapolated by solving the magnitude and phase Bode equations for the magnitude and phase values at 10 Hz. In this fashion, a complete equation for the impedance as a function of frequency can be written for every measured condition.

An inspection of the calculated impedance functions reveals that 1) all the poles and zeros are simple, 2) the first critical frequency is always a pole, and 3) the poles and zeros alternate. These properties imply that the impedance functions represent RC networks. A network realization of a given function is not unique. However, the problem is simplified by considering a general model [12] for microelectrodes that has proven useful to many investigators. This model is displayed in Fig. 6. The physical origin of the components is as follows.

*R<sub>m</sub>* is the resistance of the metallic portion of the microelectrode.

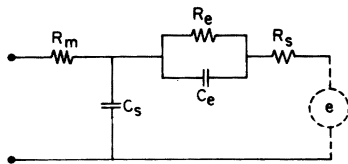


Fig. 6. General model of microelectrodes.

$C_s$  is the total shunt capacitance between the two terminals of the microelectrode from the tip to the end of the microelectrode.

$C_e$  is the polarization capacitance of an electric double layer at the interface of the metal tip and the electrolyte junction. This layer is the result of the ionic equilibrium that is established at the metal electrolyte interface.

$R_e$  is the leakage resistance due to the charged carriers crossing the electric double layer.

$R_s$  is the resistance of the electrolyte solution extending from the electric double layer to the ground terminal.

$e$  is an ideal voltage source representing the myoelectric signal.

A detailed explanation of the complicated electrochemistry of metal-liquid interfaces can be found in most textbooks of electrochemistry.

The ideal voltage source in the general model can be shorted, thus reducing the microelectrode model to a single-port network that can be reconstructed from impedance measurements.

Using the generalized model as a guide and by successive applications of the first Foster form and the first Couer form, it is possible to realize a physically significant canonic network for each impedance function. A canonic network is one that realizes a given function with a minimum number of elements, but does not necessarily provide the most physically significant network. In particular, the canonic realization yields one capacitor between the outputs of the microelectrode. However, the mechanical shunt capacitance  $C_s$  could be measured without immersing the electrode in the normal saline solution. Before the electrolytic treatment, the value of  $C_s$  was  $4.68 \pm 1.62$  pF for monopolar microelectrodes and  $4.26 \pm 1.70$  pF for bipolar microelectrodes. After the electrolytic treatment, the respective values of  $C_s$  were  $5.41 \pm 0.52$  pF and  $6.13 \pm 1.22$  pF. The difference between the capacitance of the canonic realization and  $C_s$  is represented by an electrolytic capacitance  $C_1$ . The appropriate realizations and their corresponding elements have been tabulated in Table II.

## DISCUSSION

The needle electrode described in this paper is relatively simple and inexpensive to construct. Each needle electrode requires approximately 1 h to be constructed, excluding the drying time of the epoxy cement. Over three dozen such electrodes have been made in the EMG Laboratory of the Anatomy Department at Queen's University, Kingston, Ont., Canada. None have been discarded for reasons of faulty construction.

The choice of four monopolar and six bipolar microelectrodes in each needle electrode has been extremely useful in obtaining a good recording. Fig. 7 demonstrates a comparison

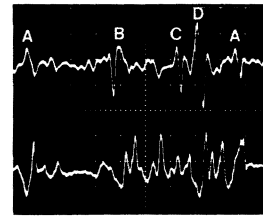


Fig. 7. Comparison of myoelectric signals simultaneously recorded with the new electrode (top trace) and a commercially available bipolar needle electrode (bottom trace). Four distinctly different motor unit potentials are easily detected in the top trace. Time scale = 5 ms/div, voltage scale = 100  $\mu$ V/div.

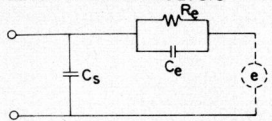
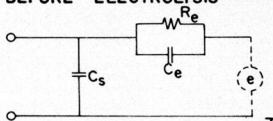
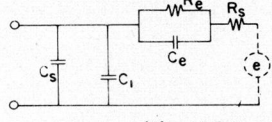
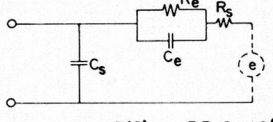
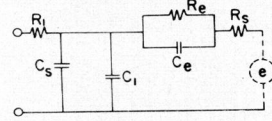
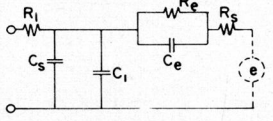
of myoelectric signals simultaneously recorded from the deltoid muscle with a typical bipolar needle electrode presently available on the market (bottom trace) and the bipolar microelectrode described in this paper (top trace). This recording was taken while the deltoid exerted maximum force. The two electrodes were placed approximately 1 cm apart along the direction of the muscle fibers. The angle and depth of insertion were identical for both electrodes. With such an arrangement, the tips of both electrodes are subjected to the electrical activity from the same muscle fibers [9]. The coincidence of the active and quiet time intervals in the two traces suggests that the two myoelectric signals were obtained from the same group of active fibers. Four distinctly different motor unit action potentials ( $A, B, C, D$ ) are easily detected in the top trace; in the bottom trace the detection of individual motor unit action potentials becomes more difficult, and in some sections it is virtually impossible.

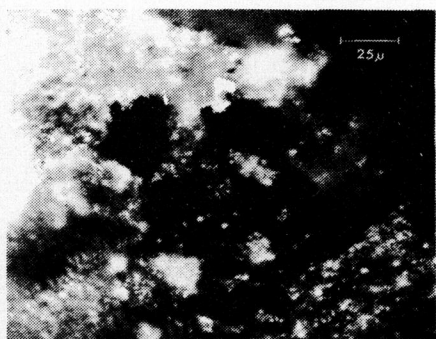
Before electrolytic treatment, the magnitude of the impedance functions of the monopolar and bipolar microelectrodes measured in normal saline solution has a slope of  $-20$  dB/decade from 10 to  $10^5$  Hz. This implies that the magnitude of the impedance decreases as  $f^{-1}$ , a relationship that varies from that of the much used bright platinum microelectrodes whose impedance magnitude at the high frequency range declines as  $f^{-1/2}$  [13]. Ten minutes after the electrolytic treatment, the impedance magnitude of the monopolar and bipolar microelectrodes was appreciably reduced and could be represented by two straight lines having the following slopes:

Monopolar Electrodes		Bipolar Electrodes	
-12.5 dB/decade	10 Hz-6 kHz	-12.5 dB/decade	10 Hz-1 kHz
-4.5 dB/decade	6 kHz-100 kHz	-4.5 dB/decade	1 kHz-100 kHz

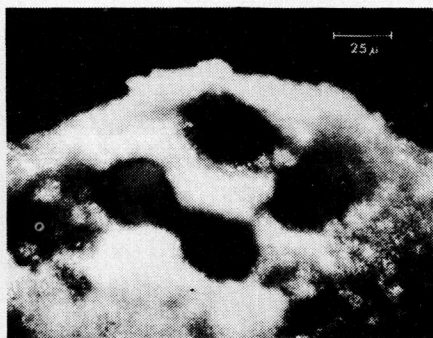
The synthesized models for the monopolar and bipolar microelectrodes are similar for each particular situation. The close proximity of the wires at the tip of the needle electrode affects the metal-electrolytic junction causing variations in the microelectrode models that cannot be easily explained. The tip of the electrode undergoes a considerable change during the electrolytic process, as can be seen in Fig. 8. The model for the untreated electrode is altered in two ways. The elements  $C_s$ ,  $C_e$ , and  $R_e$  acquire different values and new elements  $C_1$ ,  $R_s$ , and  $R_1$  appear. The resistance  $R_1$ , which appears in the same location as the resistance  $R_m$  in the general model, has a much higher value than  $R_m$ , which is approximately 400  $\Omega$ . The capacitance  $C_1$  decreases with time and the resistance  $R_s$  increases with time.

TABLE II  
MODELS FOR THE MONOPOLAR AND BIPOLAR MICROELECTRODES

MONOPOLAR ELECTRODES	BIPOLAR ELECTRODES
<p><b>BEFORE ELECTROLYSIS</b></p>  <p> <math>R_e = 1.33 \times 10^9 \Omega</math>  <math>C_s = 4.68 \text{ pf}</math>  <math>C_e = 9.72 \text{ pf}</math> </p> $Z(f) = \frac{1.33 \times 10^9}{1 + jf \cdot 0.121}$	<p><b>BEFORE ELECTROLYSIS</b></p>  <p> <math>R_e = 7.23 \times 10^9 \Omega</math>  <math>C_s = 4.26 \text{ pf}</math>  <math>C_e = 0.17 \text{ pf}</math> </p> $Z(f) = \frac{7.23 \times 10^9}{1 + jf \cdot 0.216}$
<p><b>72 HOURS AFTER ELECTROLYSIS</b></p>  <p> <math>R_s = 2.37 \times 10^6 \Omega</math>  <math>R_e = 2.28 \times 10^7 \Omega</math>  <math>C_e = 741 \text{ pf}</math>  <math>C_s = 5.41 \text{ pf}</math>  <math>C_1 = 5.19 \text{ pf}</math> </p> $Z(f) = 25.1 \times 10^6 \frac{1 + jf \cdot 10^{-2}}{(1 + jf \cdot 0.108)(1 + jf \cdot 1.54 \times 10^{-4})}$	<p><b>72 HOURS AFTER ELECTROLYSIS</b></p>  <p> <math>R_s = 3.42 \times 10^6 \Omega</math>  <math>R_e = 3.05 \times 10^7 \Omega</math>  <math>C_e = 519 \text{ pf}</math>  <math>C_s = 6.13 \text{ pf}</math> </p> $Z(f) = 33.9 \times 10^6 \frac{(1 + jf \cdot 10^{-2})}{(1 + jf \cdot 0.10)(1 + jf \cdot 1.32 \times 10^{-4})}$
<p><b>10 MINUTES AFTER ELECTROLYSIS</b></p>  <p> <math>R_i = 8.26 \times 10^4 \Omega</math>  <math>R_s = 7.04 \times 10^5 \Omega</math>  <math>R_e = 6.00 \times 10^6 \Omega</math>  <math>C_e = 2.28 \times 10^{-9} \text{ f}</math>  <math>C_s = 5.41 \text{ pf}</math>  <math>C_1 = 562 \text{ pf}</math> </p> $Z(f) = 6.77 \times 10^6 \frac{(1 + jf \cdot 10^{-2})(1 + jf \cdot 2.63 \times 10^{-4})}{(1 + jf \cdot 0.107)(1 + jf \cdot 2.00 \times 10^{-3})}$	<p><b>10 MINUTES AFTER ELECTROLYSIS</b></p>  <p> <math>R_i = 2.15 \times 10^5 \Omega</math>  <math>R_s = 1.21 \times 10^6 \Omega</math>  <math>R_e = 1.58 \times 10^7 \Omega</math>  <math>C_e = 1.21 \times 10^{-9} \text{ f}</math>  <math>C_s = 6.13 \text{ pf}</math>  <math>C_1 = 498 \text{ pf}</math> </p> $Z(f) = 17.2 \times 10^6 \frac{(1 + jf \cdot 10^{-2})(1 + jf \cdot 5.71 \times 10^{-4})}{(1 + jf \cdot 0.171)(1 + jf \cdot 2.67 \times 10^{-3})}$



(a)



(b)

Fig. 8. Tip of the electrode. (a) Before electrolysis. (b) 2 h after electrolysis. Note the formation of ridges around the electrode wires.

When normal saline is used as the electrolyte, the impedance characteristic of an untreated electrode can be controlled by three parameters: the current of electrolysis, the time duration of electrolysis, and the time lapse after the electrode has been treated. It is possible to reduce the impedance of several microelectrodes to a common value other than the minimum

value by a careful interplay of these parameters. This is a delicate manipulation that requires practice.

The major drawback of the new electrode is that minute movements of the electrode with respect to the active muscle fibers cause considerable variation in the amplitude of the recorded signal. This is a result of the small pickup area. The empirically derived voltage decrement curve [2] for myoelectric signals is

$$v_m = k \exp(-15|d|)$$

where

$d$  distance in millimeters between the origin of the myoelectric signal and the recording electrode;

$k$  maximum observed amplitude of signal in millivolts.

A movement of 100  $\mu$  away from the active muscle fiber will cause the signal amplitude to be attenuated by 80 percent. Muscle tremor becomes more dominant during strong contractions and fatigue. Yet the electrode was specifically designed to record myoelectric signals in these two states. The situation becomes somewhat paradoxical. However, the electrode remains useful because the shape of a motor unit action potential remains the same; therefore, an individual motor unit action potential train remains recognizable throughout the contraction.

**ACKNOWLEDGMENT**

The authors wish to thank technologist J. Israel for constructing the electrodes and assisting with the impedance measurements.

**REFERENCES**

[1] A. Bjork and E. Kugelberg, "Motor unit activity in the human extra-ocular muscles," *Electroencephalogr. Clin. Neurophysiol.*, vol. 5, pp. 271-278, 1953.

- [2] J. Ekstedt, "Human single muscle fiber action potential," *Acta Physiol. Scand.*, vol. 61, suppl. 226, pp. 1-96, 1964.
- [3] K. D. Wise, J. B. Angell, and A. Starr, "An integrated-circuit approach to extracellular microelectrodes," *IEEE Trans. Bio-Med. Eng.*, vol. 17, pp. 238-247, July 1970.
- [4] C. Gould, "A glass-covered platinum microelectrode," *Med. Electron. Biol. Eng.*, vol. 2, pp. 317-327, 1964.
- [5] H. A. Baldwin, S. Frank, and J. Y. Lettvin, "Glass-coated tungsten microelectrodes," *Science*, vol. 148, pp. 1462-1463, 1965.
- [6] D. H. Hubel, "Tungsten microelectrodes for recording from single units," *Science*, vol. 125, pp. 549-550, 1957.
- [7] G. Svaetichin, "Low resistance microelectrodes," *Acta Physiol. Scand.*, vol. 24, suppl. 86, pp. 5-13, 1951.
- [8] R. D. Adrain and D. W. Bronk, "Discharge of impulses in motor nerve fibers," *J. Physiol.*, vol. 67, pp. 119-151, 1929.
- [9] F. Buchthal, C. Gould, and P. Rosenfalk, "Volume conduction of the spike of the motor unit potential investigated with a new type of multielectrode," *Acta Physiol. Scand.*, vol. 38, pp. 331-354, 1957.
- [10] —, "Action potential parameters in normal human muscles and their dependence on physical variables," *Acta Physiol. Scand.*, vol. 32, pp. 200-218, 1954.
- [11] C. J. De Luca, "Myo-electric analysis of isometric contractions of the human biceps brachii," M.Sc. thesis, Univ. of New Brunswick, Fredericton, N.B., Canada, 1968.
- [12] D. A. Robinson, "The electrical properties of metal electrodes," *Proc. IEEE*, vol. 56, pp. 1065-1071, June 1968.
- [13] R. C. Gesteland, B. Howland, J. Y. Lettvin, and W. H. Pitts, "Comments on microelectrodes," *Proc. IRE*, vol. 47, pp. 1856-1862, Nov. 1959.

# Diffusion Effects of Liquid-Filled Micropipettes: A Pseudobinary Analysis of Electrolyte Leakage

C. DANIEL GEISLER, MEMBER, IEEE, EDWIN N. LIGHTFOOT, FRANK P. SCHMIDT, AND FRANCISCO SY

**Abstract**—The importance of diffusion phenomena in glass micropipettes filled with concentrated electrolyte solutions is well known. Nonequilibrium diffusion-rate equations for electrolyte-filled glass micropipettes are given for a model of situations of current interest: diffusion into an infinite medium. The solutions of these equations give the flux of material out of a micropipette as a function of time, concentration, and geometry.

## INTRODUCTION

ALTHOUGH electrolyte-filled micropipettes have proven extremely useful in electrophysiological experimentation, interpretation of potential measurements using these electrodes is subject to significant ambiguities. For one, "tip potentials" exist that may change with time or upon penetration of a cell [1]. The filtering effects of the electrical circuit to which the micropipette is attached may also be important [2]. Moreover, a liquid-junction potential exists between the electrolyte in the micropipette and the physiological fluid in which the tip is immersed [3]. The use of 3M KCl to minimize these effects is widespread. The use of this highly

concentrated KCl reduces the tip potential [4], reduces the resistance of the micropipette [1], and fixes the liquid-junction potential between the micropipette's electrolyte and axoplasm at no more than 3-4 mV [3].

The resulting difference in concentrations between the micropipette electrolyte and the less-concentrated ionic environment into which the micropipette is inserted will cause an outward diffusion of electrolyte. The effects of such diffusion may alter the external ionic environment and thus are of concern [5]. Such diffusion effects have in fact been experimentally demonstrated for molecules such as acetylcholine [6]. Electrolyte diffusion has even been used as an intracellular marking technique: while recording intracellularly, Harris *et al.* [7] used diffusion of Niagara Sky Blue dye from the recording electrode to mark the penetrated cells.

Quantitative descriptions of diffusion rates from micropipettes are not common in the literature, but a steady-state solution has been obtained by Nastuk and Hodgkin [8] and by Krnjević *et al.* [6]. It is the purpose of this paper to present a more general, time-dependent description of electrolyte diffusion.

## ANALYSIS

Since the geometry of experimental systems is quite variable, and frequently not known in detail, it is desirable to consider simplified models for possible limiting cases. We consider here

Manuscript received April 12, 1971; revised November 8, 1971.

C. D. Geisler is with the Department of Electrical Engineering and the Laboratory of Neurophysiology, University of Wisconsin, Madison, Wis.

E. N. Lightfoot, F. P. Schmidt, and F. Sy are with the Department of Chemical Engineering, University of Wisconsin, Madison, Wis.